NUMERICAL SIMULATION TO STUDY FEASIBILITY OF USING CO_2 AS A STIMULATION AGENT FOR ENHANCED GEOTHERMAL SYSTEMS

Tianfu Xu[1], Wei Zhang[2], and Karsten Pruess[1]

[1]Earth Sciences Division, Lawrence Berkeley National Laboratory, 1 Cyclotron Road, Berkeley, CA 94720
e-mail: Tianfu_Xu@lbl.gov

[2]School of Environmental Studies, China University of Geosciences, Wuhan 430074, China

ABSTRACT

A major concern in the development of enhanced geothermal systems (EGS) is achieving and maintaining adequate injectivity, while avoiding the development of preferential short-circuiting flow paths such as those caused by thermally-induced stress cracking. Past researches have tended to focus primarily on thermal and hydraulic stimulation. Recent studies suggest that chemical stimulation may improve the performance of EGS reservoirs. Geothermal injection wells are often drilled into formations containing reactive minerals such as calcite. Injecting aqueous chemical agents such as mineral acids, could be effective for mineral dissolution and porosity enhancement at distances of several meters around a well. An alternative to treatment with strong acids is the use of supercritical (SC) CO_2 as stimulation agent for an aqueous-based EGS. Reactive transport modeling is used to investigate the effectiveness of this method. We used the thermal condition and mineralogical composition from a well of Desert Peak EGS site, to examine ways in which mixtures of water and CO_2 can be injected to enhance porosity.

INTRODUCTION

The most crucial step in developing enhanced geothermal system (EGS) for commercial production is "reservoir stimulation," a process that involves injecting fluids under high pressure through boreholes deep underground, with the objective of increasing in situ fluid pressures to the point where effective normal stress on pre-existing rock fractures becomes small or negative. This will create favorable conditions for fractures to "fail in shear," meaning that one or both fracture surfaces will experience translational motion, creating a mismatch between rough surfaces that will enhance reservoir porosity and permeability.

In the early days of EGS research (1980-90s), the focus in reservoir stimulation had been almost exclusively on the geomechanical aspects of manipulating effective stress to enhance fracture permeability. Research into EGS field systems in different countries has gradually led to the recognition that chemical interactions between injected fluids and rocks can be as important as mechanical ones (Rose et al., 2007; Xu et al., 2009; Portier et al., 2009). Removal of silica and calcite scaling from wellbores is commonly accomplished by injecting strong mineral acids, such as HCl (Mella et al., 2006). Injected strong acid tends to enter the formation via the first fluid entry zone, dissolving first-contacted minerals aggressively while leaving much of the rest of the wellbore untreated. The effect of calcite dissolution using chelating agents is better than mineral acids, but still quite aggressive (Xu et al., 2009).

In the present paper, we explore the feasibility of using supercritical CO_2 as a stimulation agent for enhanced geothermal systems (Rosenbauer et al., 2005). This may offer the ancillary benefit of storing some amounts of greenhouse gas in geologic formations. The thermal and geochemical conditions at Desert Peak EGS site were used. We examined ways in which mixtures of water and CO_2 can be injected to enhance porosity and injectivity. We performed thermo-hydrologic-chemical simulations in which the fractured medium was represented by a one-dimensional MINC model (multiple interacting continua; Pruess and Narasimhan, 1985), using the non-isothermal multi-phase reactive geochemical transport code TOUGHREACT (Xu et al., 2006).

PROBLEM SETUP

Geometric configuration and flow parameters

The MINC (multiple interacting continua) method was employed for a fractured geothermal reservoir (Figure 1). MINC is designed to resolve “global” flow and diffusion of chemicals in the fractured rock and its interaction with “local” exchange between fractures and matrix rock. This method was first developed by Pruess and Narasimhan (1985) for fluid and heat flow in fractured porous media. The extension of the MINC method to reactive geochemical transport is described in detail by Xu and Pruess (2001). In the case of reactive chemistry, diffusive fluxes may be controlled by reactions occurring near the fracture walls. The resolution of concentration gradients in matrix blocks is achieved by appropriate subgridding. In the present study, subgrid 1 represents the fracture vein alteration. Subgrids 2 and 3 represent the rock matrix. The MINC concept is based on the notion that changes in fluid pressures, temperatures and chemical concentrations propagate rapidly through the fracture system, while invading the tight matrix blocks only slowly. Therefore, changes in matrix conditions will be (locally) controlled by the distance from the fractures and can then be modeled by means of one-dimensional strings of nested grid blocks.

We consider an idealized fractured porous medium with two perpendicular sets of plane, parallel fractures of equal aperture and spacing. Because of the assumed symmetry only one column of matrix blocks needs to be modeled. Our conceptual model considers a one-dimensional flow tube between injection and production well, which should be considered as a small sub-volume of a much more extensive 3-D reservoir. From the injection to the production side, the model consists of 72 grid blocks representing 600 m distance. The block size gradually increases from 0.1 m at the injection side to 20 m at the production side.

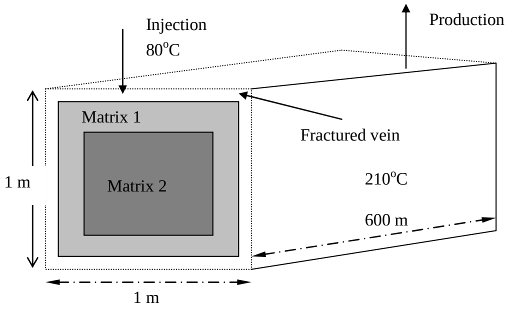

Figure 1: Subgridding in the "multiple interacting continua" (MINC) method. The figure represents a view of a rock matrix column that is bounded by fractures.

Hydrological parameters used in the present simulations are listed in Table 1. Even though we took thermal and mineralogical data from the Desert Peak (DP) site as a starting point, we attempted to use thermophysical conditions and parameters that could represent general geothermal reservoirs. An initial reservoir temperature of 210°C was used, an initial hydrostatic pressure of 200 bars was assumed for about 2000 m depth, and both were taken from Xu et al. (2009) for chemical stimulation of the DP case.

Initial water chemical compositions for the fractured vein and matrix were obtained by equilibrating a dilute water with their corresponding mineral compositions (Table 2) at a temperature of 210°C. Different mixtures of CO_2 and water were injected (see below). A distill water with a base-case temperature of 80°C, representing steam condensate, was used for injection. Conductive heat exchange with the surrounding low-permeability rock is an important process, and is treated with a semi-analytical technique developed by Vinsome and Westerveld (1980).

Table 1: Hydrogeological and thermal parameters used for the three continua (a density of 2650 kg.m^{-3}, a heat capacity of 1000 J.kg^{-1} K^{-1}, and a diffusivity of 1×10^{-9} m^2.s^{-1} were used for all three).

Parameters	Fractured	Matrix 1	Matrix 2
Volume fraction	10%	20%	70%
Permeability (m^2)	1×10^{-11}	2×10^{-18}	2×10^{-18}
Porosity	0.3	0.05	0.05
Thermal conductivity (W.m^{-1} K^{-1})	2.9	3	3
Tortuosity	0.5	0.05	0.05

Mineralogical composition

In our model, the mineralogical composition was defined based on pre-Tertiary unit 2 (pT2) from well DP 23-1, which is a quartz monzodiorite with quartz, plagioclase, and potassium feldspar (Lutz et al., 2004). A clinopyroxene and hornblende-bearing diorite directly overlies the main granodiorite intrusive body. The diorite is medium crystalline and contains primary hornblende phenocrysts with cores of clinopyroxene. The diorite is strongly propylitically altered to epidote, chlorite, pyrite and calcite, is moderately sericitized, and has also been thermally metamorphosed by the underlying granodiorite intrusive. Initial mineralogical composition used in the modeling is summarized in Table 2. Fracture vein was specified with a larger volume fraction of calcite (20% over 4%). Rock matrix was specified with a larger volume fraction of quartz (25% over 9%). Plagioclase (a solid solution) was modeled using two end-members of 50% low-albite and 50% anorthite. Dolomite, siderite, and ankerite could be formed after CO_2 injection and are specified as secondary minerals in the simulations.

Mineral dissolution and precipitation are considered under kinetic conditions. A general kinetic rate law was used, which can be found in Xu et al. (2009). Table 3 lists parameters for the kinetics of mineral reactions used in the model, which were taken from Xu et al., (2007, 2009).

Table 2: Initial mineralogical composition of fracture zone and rock matrix used in the simulations, after Xu et al. (2009).

Mineral	Fracture vein (Volume fraction, %)	Matrix (Volume fraction, %)
Quartz	**9**	**25**
Calcite	**20**	**4**
Low-Albite	21.5	21.5
Anorthite	21.5	21.5
K-Feldspar	13	13
Chlorite	8	8
Illite	7	7
Others	8	8

Table 3: List of kinetic rate parameters for minerals considered in the simulation (n = 0 for neutral mechanism, n > 0 for acid mechanism).

Mineral	k_{25} (moles $m^{-2}s^{-1}$)	E_a (KJ/mol)	n	Surface area (cm^2/g)
calcite	$1.55x10^{-6}$	23.5	0	9.8
	$5.01x10^{-1}$	14.4	1.0	9.8
quartz	$1.26x10^{-14}$	87.50	0	9.8
k-feldspar	$3.89x10^{-13}$	38.0	0	9.8
	$8.71x10^{-11}$	51.7	0.5	9.8
siderite	$1.26x10^{-9}$	62.76	0	9.8
	$6.46x10^{-4}$	36.1	0.5	9.8
dolomite	$1.26x10^{-9}$	62.76	0	9.8
	$6.46x10^{-4}$	36.1	0.5	9.8
ankerite	$1.26x10^{-9}$	62.76	0	9.8
	$6.46x10^{-4}$	36.1	0.5	9.8
albite-low	$2.75x10^{-13}$	69.8	0	9.8
	$6.92x10^{-11}$	65.0	0.46	9.8
anorthite	$2.75x10^{-13}$	69.8	0	9.8
	$6.92x10^{-11}$	65.0	0.46	9.8
illite	$1.66x10^{-13}$	35.0	0	151.6
	$1.05x10^{-11}$	23.6	0.34	151.6
chlorite	$3.02x10^{-13}$	88.0	0	151.6
	$7.76x10^{-12}$	88.0	0.5	151.6

Simulation setup

Two groups of eleven simulations were performed using different combinations of injection patterns, rates, temperatures, mineral reactive areas, and simulation times. Group one was carried for screening calculations (Table 4). We started from injecting 0.01kg/s CO_2 for 1 day, then injecting 0.1 kg/s water for another one day. In other four simulations in Group one, injection of both water and CO_2 at the same time was applied for a period of one day. Case 2 injected 0.1 kg/s water and 0.01 kg/s CO_2 (10% of water injection). Cases 3, 4, and 5 injected the same amount of water (0.1 kg/s), but different amounts of CO_2, or 7.5%, 5.15%, and 5.1%, respectively. The 5.1% CO_2 co-injection in Case 5 can just all dissolve into water. With the 5.15% CO_2 injection in Simulation 4, two-phase conditions with small gas saturation were formed.

Case 3 was selected as a base to further investigate the sensitivity regarding injection rate, temperature and reactive area (Group 2, Table 5). A longer period of simulation time of 10 days was applied. Case 6 used an injection temperature of 80^{o}C, reactive surface areas as given in Table 3, and injection of 0.1 kg/s water and 7.5% CO_2. Cases 7 and 8 changed the injection temperature 80^{o}C (in Simulation 6) to 60 and 40^{o}C, respectively. Case 9 used a surface area decreased by one order of magnitude (from Table 3). Case 10 used a surface area increased by one order of magnitude. Case 11 doubled the injection amount of water and CO_2 (0.2 kg/s water with 7.5% CO_2).

Numerical simulations were done with the non-isothermal reactive geochemical transport program TOUGHREACT, whose physical and chemical process capabilities and solution techniques have been discussed by Xu and Pruess (2001). The program can be applied to one-, two-, or three-dimensional porous and fractured media with physical and chemical heterogeneity, and can accommodate any number of chemical species present in liquid, gas and solid phases. A broad range of subsurface thermal-physical-chemical processes are considered under various thermohydrological and geochemical conditions of pressure, temperature, water saturation, ionic strength, and pH and Eh. Changes in porosity are monitored from changes in mineral volume fractions.

Table 4: List of Group one simulations with different specifications

Simulation (Case)	Injection	Remark
1	Inject 0.01kg/s CO_2 for 1 day, then inject 0.1 kg/s water for 1 day	Sequential
2	Inject 0.01 kg/s (10% of water injection) CO_2 and 0.1 kg/s water at the same time for another 1 day	Co-injection
3	**(0.1 kg/s water with) 7.5% CO_2**	Co-injection, **Base for Group 2**
4	5.15% CO_2	Co-injection
5	5.1% CO_2 (all dissolved)	Co-injection

Table 5: List of Group two simulations with different injection rate, temperature and reactive area using a simulation time of 10 days.

Simulation (Case)	Injection temperature	Reactive surface area	Injection rate
6, base-	80^{o}C	Table 3	0.1 kg/s water (with 7.5% CO_2)
7	60^{o}C		
8	40^{o}C		
9		Decreased by one order of magnitude	
10		Increased by one order of magnitude	
11			0.2 kg/s water (with 7.5% CO_2)

RESULTS AND DISCUSSION

Figure 2 shows change of porosity along the fracture vein obtained with five simulation cases in Group one (after one day for Cases 2-5; but after two days for the sequential case). Sequential injection of CO_2 and water results in a very small porosity enhancement. Four cases of co-injection of water and CO_2 result in a much larger porosity enhancements than the sequential case because both calcite dissolution (discuss later) and transport of dissolved chemical constituents need water. Results from the four co-injection cases are similar as long as injection amount of CO_2 can promote a small two-phase condition. All CO_2 in the case of 5.1% can just completely dissolve into water. Therefore, co-injection cases were identified to further study, and the case with injection of 0.1 kg/s water and 7.5% CO_2 was selected for sensitivity simulations designed in Group two. The result sensitivities are discussed below.

The higher injection temperature causes more porosity increases close to the injection point, but it extends into a short distance (Figure 3). For injection fluids with an 80^{o}C temperature, porosity increases to 0.36 from 0.3 close to the injection point, and penetrates about 18 m. While, for a 40^{o}C temperature, porosity increases to 0.332 close to the injection point, but extends more than 40 m. The higher reaction rate (through surface area) causes more porosity increases close to the injection point, but it extends a short distance (Figure 4). For surface areas increased by one order of magnitude (from values in Table 3), porosity increases to 0.42 from 0.3 close to the injection point, and extends about 8 m. While, for areas decreased by one order of magnitude, porosity increases to 0.308 close to the injection point, but penetrates more than 80 m. An increase in injection rate results in a decrease in porosity enhancement close to the injection point, but it extends into a longer distance (Figure 5).

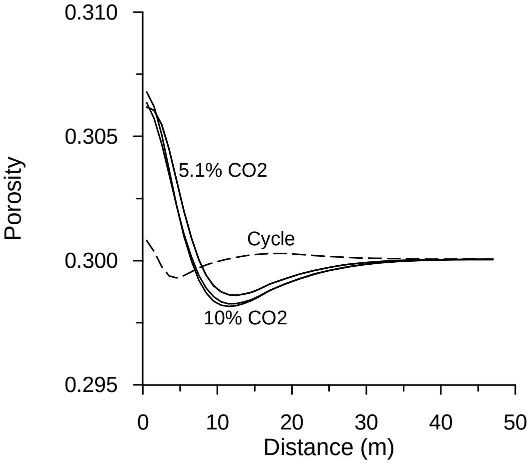

Figure 2: Change of porosity along fracture vein after one day simulation (but after two days for the case of sequential, injecting CO_2 for one day and then injecting water for another one day). Initial porosity is 0.3.

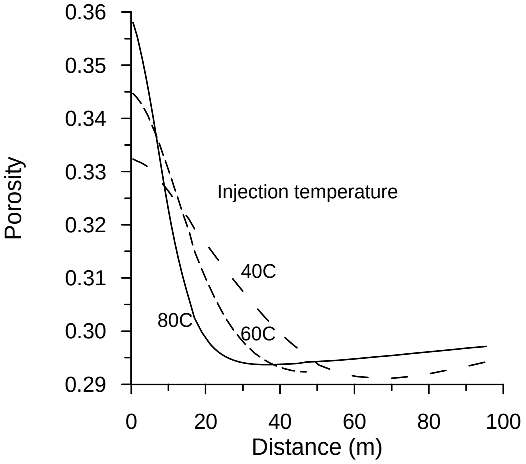

Figure 3: Change of porosity along fracture vein obtained with different injection temperatures after a simulation time of 10 days.

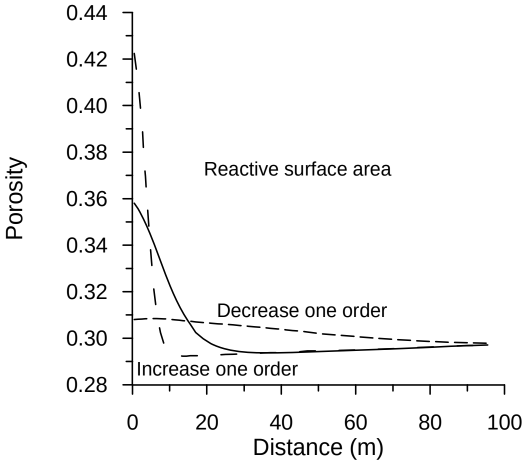

Figure 4: Change of porosity along fracture vein obtained with different reactive surfaces after a simulation time of 10 days (80°C injection temperature).

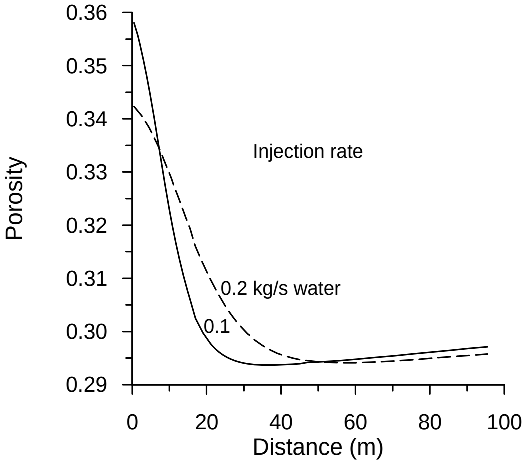

Figure 5: Change of porosity along fracture vein obtained with different injection rates after a simulation time of 10 days.

Changes of porosity are due to dissolution and precipitation of minerals. Let us use Case 6 (injection of 0.1 kg/s water with 7.5% CO_2) as example to illustrate alteration of minerals induced by the co-injection of CO_2. Porosity enhancement mainly results from calcite dissolution (Figure 6). Porosity increases significantly with time close to the injection point (with about 6% after 10 days), and extends with distance. A slight calcite precipitation was obtained at the front due to temperature increase, because calcite solubility decreases with temperature. The temperature profiles along fracture vein are presented in Figure 7. A small amount of albite-low dissolves at the front (Figure 8). Similar dissolution pattern was observed for anorthite. Both minerals are end-members of plagioclase (a solid solution). The corresponding changes of porosity along the fracture vein at different times are presented in Figure 9.

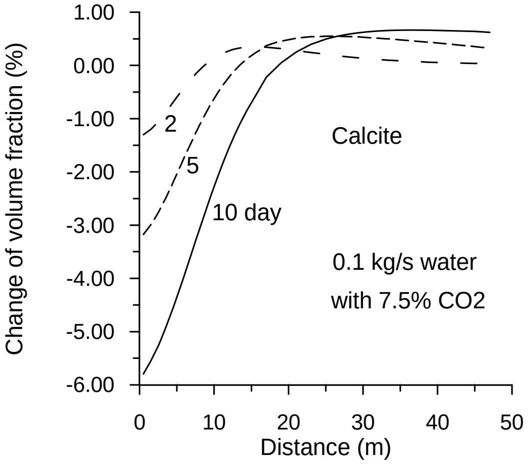

Figure 6: Change of calcite volume fraction along fracture vein at different times with Simulation 6.

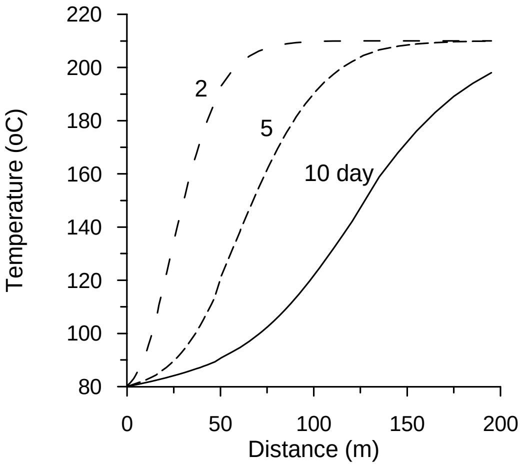

Figure 7: Temperature profiles along fracture vein at different times with Simulation 6.

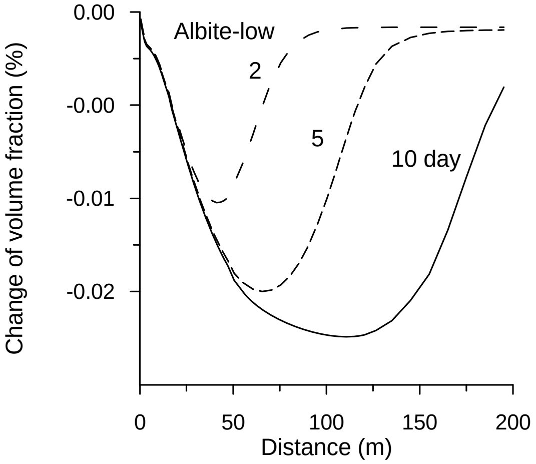

Figure 8: Change of albite-low volume fraction along fracture vein at different times with Simulation 6.

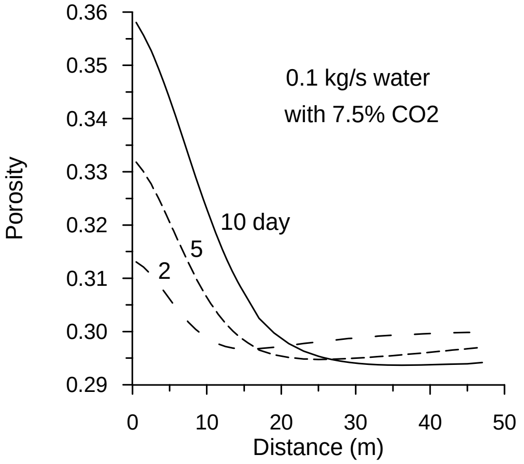

Figure 9: Change of porosity along fracture vein at different times with Simulation 6 (base-case of Group 2).

CONCLUSIONS

Chemical stimulation using CO_2 has been explored by numerical modeling using thermal conditions and mineral composition from the Desert Peak EGS site. Sequential injection of CO_2 and water results in a very small porosity enhancement. Co-injection of water with SC CO_2 results in much stronger porosity enhancement around an injection well. This is because both mineral dissolution and transport of dissolved chemical constituents need water. Results from several co-injection cases with different portion of CO_2 relative to water (5-10%) are similar as long as the amount of CO_2 can promote a small two-phase condition or just meets its solubility in water. Increases in porosity mainly result from calcite dissolution. Many thermophysical and chemical factors affect calcite dissolution and associated enhancement in formation porosity, including injection temperature, mineral abundance and distribution, reaction kinetics, and injection rate. Favorable conditions are low injection temperature, large injection rate, and slow reaction rates, which could result in moderate porosity enhancement close to the injection well, but extending a long distance into the formation.

ACKNOWLEDGEMENTS

This work was supported by the Assistant Secretary for Energy Efficiency and Renewable Energy, Office of Geothermal Technologies, of the U.S. Department of Energy, under Contract No. DE-AC02-05CH11231 with Lawrence Berkeley National Laboratory (LBNL). The second author (Wei Zhang) of this paper was supported by National Natural Science Foundation of China (NSFC, No. 40872158). The support provided by LBNL during a visit of Wei Zhang to Berkeley is acknowledged.

REFERENCES

Lutz, S.J., A.R. Tait, and C.L. Morris, 2004. Stratigraphic relationships in mesozoic basement rocks at the Desert Peak east EGS area, Nevada, In Proceedings of Twenty-Ninth Workshop on Geothermal Reservoir Engineering, Stanford University, Stanford, California.

Mella, M., Kovac, K., Xu, T., Rose, P., Mcculloch, J., Pruess, K., 2006. Calcite dissolution in geothermal reservoirs using chelants, In Proceedings of Geothermal Resources Council.

Narasimhan, T.N., Witherspoon, P.A., 1976. An integrated finite difference method for analyzing fluid flow in porous media, Water Resour. Res. 12, 57–64.

Portier, S., Franc¸ Vuataza, F.D., Namib, P., Sanjuanc, B., Gérardd, A. 2009. Chemical stimulation techniques for geothermal wells: experiments on the three-well EGS system at Soultz-sous-Forêts, France. *Geothermics*, 38, 349-359.

Rose, P., T. Xu, K. Kovac, M. Mella, and K. Pruess, 2007. Chemical stimulation in near-wellbore geothermal formations: silica dissolution in the presence of calcite at high temperature and high pH, In Proceedings of Thirty-Second Workshop on Geothermal Reservoir Engineering, Stanford University, Stanford, California, January 22-24, 2007.

Rosenbauer, R.J., T. Koksalan, J.L. Palandri, 2005. Experimental investigation of CO_2-brine-rock interactions at elevated temperature and pressure: Implications for CO_2 sequestration in deep-saline aquifers. *Fuel Processing Technology*, 86, 1581-1597.

Vinsome, P. K. W., and Westerveld, J., 1980. A simple method for predicting cap and base rock heat losses in thermal reservoir simulators. J. Canadian Pet. Tech., 19 (3), 87–90.

Xu, T., and Pruess, K., 2001. Modeling multiphase non-isothermal fluid flow and reactive geochemical transport in variably saturated fractured rocks: 1. Methodology. *Am. J. Sci*., 301, 16-33.

Xu, T., Sonnenthal, E.L., Spycher, N., Pruess, K., 2006. TOUGHREACT - A simulation program for non-isothermal multiphase reactive geochemical transport in variably saturated geologic media: Applications to geothermal injectivity and CO_2 geological sequestration, *Computer & Geoscience*, v. 32/2 p. 145-165.

Xu, T., J. A. Apps, K. Pruess, and H. Yamamoto, Numerical modeling of injection and mineral trapping of CO2 with H2S and SO2 in a sandstone formation, *Chemical Geology*, v. 242/3-4, p. 319-346, 2007.

Xu, T., Rose, P., Fayer, S., Pruess, K., On modeling of chemical stimulation of an enhanced geothermal system using a high pH solution with chelating agent, Submitted to *Geofluid*, v. 9, p. 167-177, 2009.